Interaction Notes

Note 329

24 June 1977

Singularity Expansions for Cylinders of Finite Conductivity

P. Vincent

Laboratoire d'Optique Electromagnétique
Equipe de Recherche associée au C. N. R. S.
Faculte des Sciences et Techniques
Centre de St-Jérôme
13397 Marseille Cedex 4, France

7 FEB 1978
Technical Library
AF Weapons
Laboratory

ACKNOWLEDGMENT

The author is grateful to Professor R. Petit who encouraged this work, to Professor M. Cadilhac for helpful discussions, and Dr. M. Neviere for his constant aid.

INTRODUCTION.

The Singularity Expansion Method (SEM) has been recently introduced by C.E. Baum [1,2] in transient electromagnetics for perfect conductors. It is based on the use of the continuation of the generalized impedance matrix for complex values of the frequency. Theoretical considerations [3,4] as well as practical results [5] show that the singularities of this matrix give a good description of the time-response of the scatterer. The choice of the impedance matrix seems natural for bodies of infinite conductivity, but looks artificial when there is no surface current.

We propose here a new rigorous differential formulation to study the diffraction by arbitrary shaped cylinders made with dielectric or conducting materials which is based on the use of the scattering operator ($\mathcal{S}$-operator). It is surprising to see in the litterature that, except a few exceptions as [6], this operator is only used in theoretical considerations whereas it can be a powerful tool in numerical calculation.

Our computer program perform a direct computation of the scattering matrix, searches poles and zeros of this latter, and gives also the diffraction patterns (total cross-sections and bistatic cross-sections) for various incidences.

Because the translational invariances, we use a $\exp(i\gamma z - i\omega t)$ vectors field dependence. We examine successively the singularities in the frequency (ω) domain and in the propagation constant (γ) domain. Such complex propagation constant had been used previously in our lab to compute the coupling efficiency of grating couplers [7] or surface waves on gratings [8,9] and to exhibit a curious phenomenon of total absorption of energy. A singularity expansion, proposed in a previous paper [10], can be used to reconstruct the harmonic diffracted field.

The problem we deal with is summarized below :

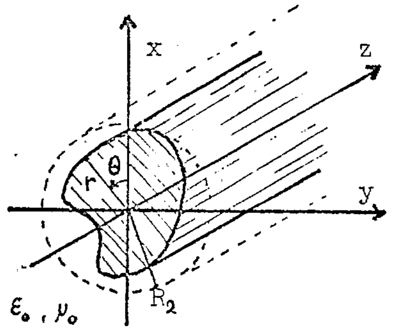

- cylindrical coordinates : r , θ , z ,
- cylinder : . axis Oz ,
  . arbitrary shape (can be inhomogeneous)
  . infinite length,
- material : dielectric or metal (not perfect conductor),
- electromagnetic constants :
  . $\varepsilon(r,\theta)$ real or complex, independent of z and t ,
  $\varepsilon = \varepsilon_0$ for $r > R_2$,
  . $\mu = \mu_0$ in all space† .

<u>Notations</u> :

$\vec{k}$ is the wave vector ($|\vec{k}| = k = 2\pi/\lambda$; λ = wavelength),
γ is its projection on Oz ; $\tilde{k}$, on xOy ,
$\phi = (\overrightarrow{Oz},\vec{k})$.

I - THE SCATTERING OPERATOR.

When the distance r to axis Oz of the cylinder tends to infinity, it is possible to separate the electromagnetic field in two parts : the incoming waves ψ^- and the outgoing ones ψ^+. When the scattering obstacle is removed, we note the outgoing wave ψ_0^+. The linearity of Maxwell equations implies there exists a linear operator such as :

$$(1) \qquad \psi^+ = \mathcal{S}\, \psi_0^+ .$$

It is worthnoting that usual definition of the scattering operator [11] uses ψ^- instead of ψ_0^+. Our definition is chosen because it gives a unity operator when the obstacle is removed. It is not the case for the usual one because of the phase change of a convergent cylindrical wave when passing through a focus.

It is very interesting in view of numerical applications, to use a representation of the $\mathcal{S}$ operator which is as much as possible independent of the incident field structure.

We assume here that our diffraction problem is invariant with respect to arbitrary translations of the time coordinate t and of the spatial coordinate z . It is easy to show [12] that these properties implie the conservation of the frequency $\omega/2\pi$ and of the projection γ of the wave vector $\vec{k}$ on Oz axis. Thus we use complex amplitudes for the field, assuming an $\exp[i(\gamma z - \omega t)]$ dependence.

.../.

† This restriction is only for convenience ; it could be removed immediately at the price of a little more computation time.

The electromagnetic field may be expressed in terms of its transverse and axial components :

$$(2)\ \begin{cases} \vec{E}(r,\theta,z,t) = \mathrm{Re}\ \{(\vec{E}_T(r,\theta) + E_z(r,\theta)\vec{e}_z)\ \exp\ [i(\gamma_z - \omega t)]\}\ , \\ \vec{H}(r,\theta,z,t) = \mathrm{Re}\ \{(\vec{H}_T(r,\theta) + H_z(r,\theta)\vec{e}_z)\ \exp\ [i(\gamma_z - \omega t)]\}\ , \end{cases}$$

and it is well known [13] that the transverse components ($\vec{E}_T$, $\vec{H}_T$) can be derived from the axial ones (E_z , H_z).
The latters are solutions of propagation equations established in annex A, and must be considered as generalized functions or distributions.

When $r > R_2$, $\varepsilon = \varepsilon_0$ and $\mu = \mu_0$; then we can write the field in terms of Hankel functions. Let us define :

$$\tilde{k}_0{}^2 = \omega^2\varepsilon_0\mu_0 - \gamma^2\ ,$$

$$Z_0 = 120\ \pi = \sqrt{\frac{\mu_0}{\varepsilon_0}}\ ,$$

$\tilde{H}_n^{\pm}(\tilde{k}_0 r) = \exp\left[\pm i(n + \frac{1}{2})\frac{\pi}{2}\right] H_n^{\pm}(\tilde{k}_0 r)$ where $H_n^{\pm}$ are the Hankel functions corresponding to n order. We get :

$$(3)\ \begin{cases} E_z(r,\theta) = \sum\limits_n (e_n^- \tilde{H}_n^-(\tilde{k}_0 r) + e_n^+ \tilde{H}_n^+(\tilde{k}_0 r))\ \exp(in\theta)\ , \\ Z_0\ H_z(r,\theta) = \sum\limits_n (h_n^- \tilde{H}_n^-(\tilde{k}_0 r) + h_n^+ \tilde{H}_n^+(\tilde{k}_0 r))\ \exp(in\theta)\ . \end{cases}$$

When r tends to infinity, the functions $\tilde{H}_n^{\pm}(\tilde{k}_0 r)$ are equivalent to $\exp(\pm i\tilde{k}_0 r)/\sqrt{\tilde{k}_0 r}$. Thus the angular dependence of the outgoing field is characterized by the functions :

$$(4)\ \begin{cases} E_z^+(\theta) = \sum\limits_n e_n^+ \exp(in\theta)\ , \\ Z_0\ H_z^+(\theta) = \sum\limits_n h_n^+ \exp(in\theta)\ , \end{cases}$$

which are periodic with period 2π , square-integrable over one period, and so belong to the Hilbert space $L_2(2\pi)$.

Since the electromagnetic field is completely determined by its axial components $E_z(r,\theta)$ and $H_z(r,\theta)$, the diffraction operator works on the Hilbert space $L_2(2\pi) \oplus L_2(2\pi)$ (where $\oplus$ is the direct sum) , whose elements are column vectors of the form :

$$(5)\qquad \psi^+ = \begin{bmatrix} E_z^+(\theta) \\ Z_0\ H_z^+(\theta) \end{bmatrix}\ .$$

Using the Dirac notation, we write $|n\ 1>$ for $\begin{bmatrix} \exp(in\theta) \\ 0 \end{bmatrix}$ and $|n\ 2>$ for $\begin{bmatrix} 0 \\ \exp(in\theta) \end{bmatrix}$. The matrix elements are :

$$S_{m,p}^{n,q} = <n\ q|\ \mathcal{S}\ |m\ p> \quad \begin{cases} m,n \in Z^{\dagger} \\ p,q \in \{1,2\} \end{cases}.$$

.../.

† Z is the set of relative integers (positive, negative, or equal to zero integers).

If the obstacle is removed, the outgoing field coefficients in expansion (3) can be derived in a straightforward manner from the coefficients e_n^- , h_n^-) of the incoming field. Thus, our S-matrix also gives the outgoing field coefficients (e_n^+ , h_n^+) from the incoming ones (e_n^- , h_n^-) . The property is used for the computation of the S-matrix (Annex C) .

II - PROPERTIES OF THE S-MATRIX.

General properties of the diffracted field give some simple relations between the elements of the S-matrix.

II.1. Relations derived from the reciprocity theorem.

This property does not require a lossless scatterer. Annex B describes how the de Hoope's demonstration [11,14], for a finite-size diffracting structure, can be transposed to an infinite length cylinder. It is also shown that the corresponding relations between the matrix elements are :

$$(7) \qquad S_{m,p}^{n,q} = S_{-n,q}^{-m,p} \quad .$$

II.2. Relations from the energy conservation.

Of course this only holds for lossless dielectrics or perfect conductors. Using the time-dependence in $\exp(-i\omega t)$ we note $\vec{E}^+$ and $\vec{H}^+$ the complex vectors associated with the outgoing field.

Lemma :

Given a circular cylinder $\mathcal{C}_2$ (axis Oz , radius R_2) with $\varepsilon = \varepsilon_0$ and $\mu = \mu_0$ outside $\mathcal{C}_2$, it is shown (annex B) that two diffracted field ψ^+ and ψ'^+ verify :

$$(8) \qquad \frac{1}{2}\iint_{\mathcal{C}_2} (\vec{E}^+ \wedge \overline{\vec{H}'^+})\vec{n}\, ds = \frac{2\omega\varepsilon_0}{\tilde{k}_0^2} \sum_n (e_n^+ \overline{e_n'^+} + h_n^+ \overline{h_n'^+}) \ ,$$

where $\bar{e}$ is the complex conjugate of e .

The right side of (8) is the scalar product of ψ^+ and ψ'^+ in $L_2(2\pi) \oplus L_2(2\pi)$. Thus we write :

$$\frac{1}{2}\iint_{\mathcal{C}_2} (\vec{E}^+ \wedge \overline{\vec{H}'^+})\vec{n}\, ds = C <\psi'^+,\psi^+> \ ,$$ where C is a normalisation constant.

In particular, if $\psi'^+ = \psi^+$, the energy flux of the outgoing field $C <\psi^+,\psi^+>$ is proportional to the square of the norm $||\psi||$. The result is that, for a lossless scatterer, the S-matrix does not change the norm of the vectors, and consequently, everywhere its inverse exists, the S-matrix is unitary.

II.3. *Relations from the symmetries of the scatterer.*

The symmetries of the scatterer give various relations between the matrix elements, which may be useful to check the validity and the accuracy of numerical results. For example, using the $\exp(in\theta)$ basis :

a) if xOz is a plane of symmetry, we get :

$$S^{n,q}_{m,p} = S^{-n,q}_{-m,p} \quad ; \tag{9}$$

b) if yOz is a plane of symmetry :

$$S^{n,q}_{m,p} = (-1)^{n-m} \; S^{-n,q}_{-m,p} \quad ; \tag{10}$$

c) if Oz is an axis of symmetry (order 2) :

$$S^{n,q}_{m,p} = (-1)^{n-m} \; S^{n,q}_{m,p} \quad . \tag{11}$$

The latter formula shows that the one over two parallel to the main diagonal of the matrix are zero. This is in agreement with the remark of paragraph III.5.

III – ANALYTIC CONTINUATIONS OF THE S-MATRIX AND THEIR SINGULARITIES.

As it will be shown later, an interesting problem is to study the analytic continuations of the S-matrix for complex values of different variables.

Because the translational invariance, $\mathcal{S}$ is an operator-valued function of γ and $k_0 = \omega\sqrt{\varepsilon_0\mu_0}$. The definitions of the incoming and outgoing waves are obvious for real values of the variables, but it is not the same when the variables are complex. Let us assume that there is no ambiguity in the definition of $\mathcal{S}$, which implies the use of appropriate branch cuts ; if such branch cuts are used, we assume that they do not lie between the singularities and the segment of the real axis we are dealing with.

III.1. *Continuation in the frequency domain.*

We assume k_0 complex and γ a given real number. The study is suggested by the presence of resonance peaks in the cross-section curves versus frequency. For a given scatterer, the peaks always appear, for the same frequency, whatever the angle θ of incidence. This suggests to relate such resonances with singularities of the S-matrix in the complex frequency plane.

We will not try to give here a rigorous mathematical basis for this continuation. But the comparison of the harmonic diffrected field computed directly, or reconstructed by means of singularities expansions, enables us to check the validity of our hypothesis. It seems not hazardous to assume that, outside a discrete spectrum and for $\mathrm{Re}(k) > 0$, the $\mathcal{S}$-operator has an inverse.

Let us introduce the eigenvectors $|i\ j>$ of S^{-1} and the eigenvalues c_i :

$S^{-1}\ |i\ j> \ = \ c_i\ |i\ j>$, where the subscript j is used for degenerate eigenvalues.

We assume that S is regular enough to use the decomposition :

$$(12) \qquad S = \sum_{i,j} \frac{|i\ j> <i\ j|}{c_i} ,$$

where $<i\ j|$ is an eigencovector of S^{-1} for c_i such as :

$<i\ j|l\ m> \ = \ \delta_{i,l}\ \delta_{j,m}$ ($\delta_{i,l}$ is the Krönecker symbol).

The poles of S are the values of k that reduce the eigenvalue $c_i(k)$ to zero : they are given by the roots of equations:

$$(13) \qquad c_i(k) = 0 .$$

Let us now assume that the poles are simple, i.e. the roots of equation (13) are of first order. This hypothesis can be understood if we remember that a perfectly conducting shpere has only simple poles [15] and it seems likely that the same thing applies for finite-size objects. Our two dimentional problem is similar because it has a finite-size cross-section.

Then, the residue of the S-matrix for the pole k_l is defined by :

$$(14) \qquad R_l = \lim_{k \to k_l} (k - k_l)\ S(k) .$$

Assuming that the transition operator $\mathcal{E} = \mathcal{S} - 1$ is compact, the Fredholm analytic theorem [16] implies that R_l has a finite rank. This rank is the order of degeneracy of the resonant mode defined by the pole k_l . Let us developped the S-matrix in terms of its poles and residues :

$$(15) \qquad S(k) = \sum_l \frac{R_l}{k - k_l} + S_0(k) .$$

Equations (14) and (12) give :

$$R_l = \lim_{k \to k_l} (k - k_l) \sum_{i,j} \frac{|i\ j> <i\ j|}{c_i} ,$$

where the only contributions are obtained for $l = i$. Thus :

$$(16) \qquad R_l = \frac{dk}{dc_l} \sum_j |l\ j> <l\ j| .$$

The residues are matrices (dyadics) given by the eigenvectors and covectors of S for $k = k_l$, constant with respect to k . Thus the interest of this expansion for the study of transient electromagnetics is obvious. Using classical hypothesis about the asymptotic behaviour of $\mathcal{S}(k)$, we may know the time dependent electric field by means of a contour integral in the complex k plane : this is the classical SEM [2]. Residue theorem implies that the regular part $S_0(k)$ of the S-matrix does not contribute to the integral : from this point of view transient response seems more easy to get than the harmonic one. But, the difficulty to determine directly the response makes the validity of expansion (15) difficult to check. In particular, the contour integral determination nescessitates the knowledge of all the poles lying inside the contour which are the roots of a transcendental equation. Thus, the number of poles is unknown, and it is very difficult to be sure to have determined all them.

This incites us to improve expansion (15) in order to be able to compute also the harmonic diffracted field. This is easy for perfect dielectrics with well separated resonances (The meaning of "well separated resonances" is given in the paragraph dealing with the symmetry properties of the modes). In practice, we must have a permittivity ε_r greater than 4 in the case of perpendicular incidence. The unitarity of the S-matrix for real values of k implies that $\det(S) = 0$ for conjugated values of the poles k_l of $S(k)$.

This property incites us to write :

$$(17) \qquad S(k) = \sum_{l=1}^{n} \frac{k - \bar{k}_l}{k - k_l} R'_l + S'_0(k) .$$

Numerical experiments have shown that the variations of $S'_0(k)$ with k are negligible provided that the discrete sum includes all the poles lying near the segment of the real axis we are concerned with to obtain the harmonic response, this expansion will be used in a limited frequency domain. $S'_0(k)$ is a quasi-constant matrix which gives the contribution of singularities lying outside this domain.

III.2. Continuation to complex propagation constant γ .

Let us now assume that k_0 is given and real, ε is real and γ is allowed to be complex. If a pole γ_p of $\mathcal{S}$ lies on the real axis, this means that there is a solution to Maxwell equations without incident field. In other words, if $\gamma > k_0$, the field outside the cylinder decreases when r goes to infinity : we recognize here a guided mode of the dielectric waveguide, constituted by the cylinder with axis Oz , and γ_p is the propagation constant. The eigenvector $|l\ j\rangle$ of the S-matrix describes the propagating mode.

Thus, our diffraction study enables us to determine the mode of a dielectric-waveguide of arbitrary shape.

Of course, this method also works for complex values of the permittivity ε , but then γ_p is complex. Its imaginary part gives the attenuation along Oz . If we find solution for $\mathrm{Re}(\gamma_p) < k_0$, the corresponding mode is a radiating one. Consequently, there is an attenuation along Oz , and the corresponding pole is again complex. The poles γ_p are also useful for purposes other than guided propagation. For example, if we get a space-packet of incident waves :

$$\tilde{\psi}^i(z) = \int_{\gamma_1}^{\gamma_2} \psi^i(\gamma)\, e^{i\gamma z}\, d\gamma ,$$

we can determine the response of the scatterer as we did for grating-couplers in [7].

III.3. *Continuation to complex angular constant* α .

The two preceding ways to do the analytic continuation of the S-matrix was obvious. The way proposed here is less intuitive. The equations are invariant if we change θ in $\theta + 2\pi$. This implies (Floquet's theorem) that a wave having an $\exp(i\alpha\theta)$ dependence is coupled only to $\exp[i(\alpha + n)\theta]$. Physical reasons imply that for finite cross-section cylinders, α can only be an integer. But we may consider the continuation of the S-matrix to complex values of α : this is done by radio-engineers who study the propagation over the earth [17] with the use of Watson transform. This is also employed in quantum theory of scattering by people dealing with the Regge poles [12].

For us, the interest of such a procedure appears when the incident field imposes the values of γ and k_0 . The localization of the poles α_p allows us to predict the occurence of a resonance when α_p is near in integer value. Of course, α_p is an integer when we are in guided-propagation conditions and become complex when γ is smaller than k . If α_p is near the real axis, we have a radiating mode, but we can consider that it is induced by rotating wave. It is the same has in the preceding paragraph, when we consider complex propagation constants γ ; for small section, it seems that the propagation along Oz is more important than the rotation around Oz , but for large radius of curvature, the rotation is an interesting point of view and lead to "creeping-waves" [18].

III.4. *Searching poles and computing residues.*

Numerical difficulties could arise if the determination of the poles is conducted with the S-matrix, and are avoided if we use its inverse S^{-1} . This could be done very simply, inverting outgoing and incoming conditions, so the program computes directly the inverse matrix. The poles are the roots of equation :

$$\det(S^{-1}) = 0 .$$

Thus, we have to found the zeros of a complex function of complex variable. This could be done by an iterative method using a linear approximation as we do in this program, or as we did for grating-couplers [7] using an homographic approximation.

The residues are given by the eigenvectors of S . For a dielectric cylinder the S and S^{-1} matrices are unitary, so all the eigenvalues are of modulus unity. Usual iterative methods, such as the Von Mise one, does not work with such matrices but it is possible to diagonalize the matrix $(S + S^*)/2$ (where S^* is the adjoint of S) which is hermitian by the efficient Jacobi method. Another way is to diaginalize S^{-1} , taking into account the zero eigenvalue. This could be done by elimination of superfluous equations, but nescessitates the knowledge of the main components of the eigenvector. For small matrices of order 2 or 3, an analytical solution can be exhibited. All the three methods proposed here have been used successfully in our programs.

The computation of the residues also nescessitates the determination of the derivative c_i' of the eigenvalues. This is done from the derivative $\mathcal{S}'$ of $\mathcal{S}$ using the formula :

$$c_i' = \langle i\ j | \mathcal{S}' | i\ j \rangle \ .$$

III.5. *Numerical determination of the S-matrix.*

Differential integration methods, such as the Runge-Kutta ones, allow us to compute directly the S-matrix in the $\exp(in\theta)$ basis. The equations used to this aim are given in annex C. We must emphasize that such a computation does not require much more time and memory than the direct determination of one diffracted field by one given incident field. It is only when the numbers of terms necessary to get an accurate representation of the field is great that the use of an iterative method as proposed in [19] can lead to substantial savings.

An interesting feature of our program is the use of symmetry properties of the scatterer to reduce computation requirements. Suppose that Oz is an axis of symmetry of N^{th} order (it is invariant when θ is changed in $\theta + 2\pi/N$), from Floquet's theorem a wave having an $\exp(i\alpha\theta)$ dependence is only coupled to the ones having a $\{\exp[i(\alpha + nN)\theta]\ ,\ n \in Z\}$ dependence. Consequently, it is possible to split the matrices in N independent ones of order N times smaller. The number of elementary operations is approximately proportional to the third power of the order of the matrices in a multiplication. Then for the calculation of a complete S-matrix the computation time is divide by N. Moreover we need only one sub-matrix to search a pole. Since this sub-matrix has less poles than the complete one, the iterative method used to find the pole locations work better. The computation time is then divided by N^2 .

IV – *REPRESENTATIVE RESULTS.*

IV.1. *Checking our program.*

The validity of our numerical program has been checked with various tests. The energy conservation criterion (or "optical theorem") and the reciprocity relations between matrix elements are satisfied with an accuracy of 10^{-3}.

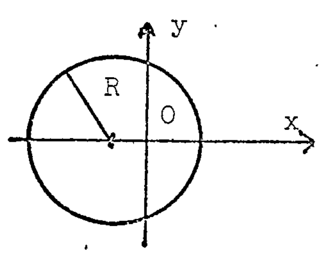

We have computed the differential cross-sections of circular cylinders, when the axis of the cylinder is shifted from Oz (figure 2). The results agree with the curves presented by Lind and Greenberg [20]. We have also writen an analytical program, using matching conditions which gives the same results.

For normal incidence, that is to say for an incident wave perpendicular to the Oz axis, the results have been compared with success to our previous programs using Noumerov algorithm [21] or integral formulation [22].

The necessity to perform a numerical integration of Maxwell equation has been proved by writing the point-matching counterpart of our program. The table 1 gives the total scattering cross section of a circular cylinder, for various shifts of its axis. When the results are good, the cross section is independent of the shift, but experiment shows that for a shift equal to half-radius, the program based on point matching method diverges before a good result is obtain. On the opposite, the numerical integration of Maxwell equations always gives the same result, for these different shifts.

N \ k_0a	0.1	0.15	0.20	0.25
13	3.495	3.565	3.741	3.927
15	3.489	3.595	3.636	3.779
17	3.487	3.501	3.564	3.716
19	3.486	3.494	3.535	12.25
21	3.465	3.800	28.20	300 000.
23	2.707	27.64		

Table 1

Total cross section of a shifted circular cylinder.

$k_0R = 0.5$
permittivity : $\varepsilon = 2.56$
oblique incidence : $\phi = 45°$
dimension of the S-matrix : N
normalized shift : k_0a .
Method used : Point-Matching .

For square or rectangular cross sections, we have computed the propagation constant of dielectric waveguides. This time, the results always agree with the values achieved by Goell [23] with a point-matching method. Several reasons can be invoked to explain the validity of cylindrical expansions in this case : the use of modified Bessel functions instead of Hankel functions outside the waveguide ; the small number of significant poles lying at the left of a given frequency with regard to the diffraction problem ; the poor sensitivity of poles location to this kind of errors.

IV.2. Poles of the square cylinder.

The poles of a square dielectric cylinder come near the real axis when the permittivity increases. This is shown in figure 3 for relative permittivity between 2 and 6. As expected, we see that the number of poles lying between the imaginary axis and a given frequency increases also with the permittivity. This may be connected with the necessity to increase the number of terms used in the Fourier series to describe the field accurately.

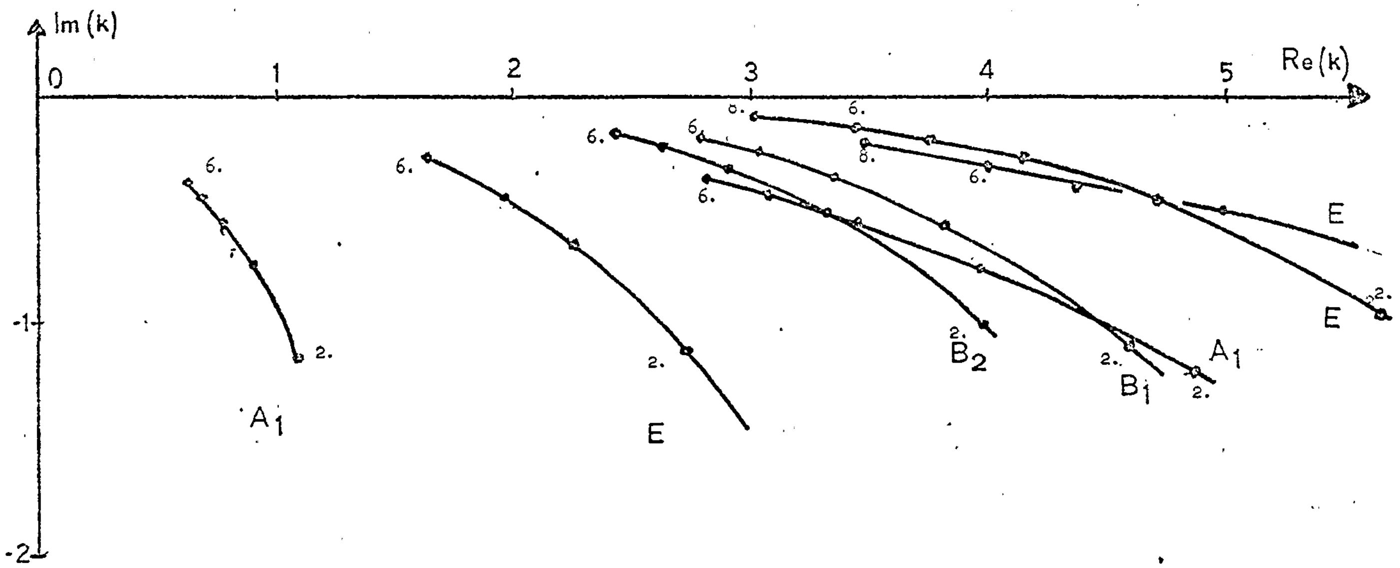

Figure 3

The locus of natural frequencies for a square lossless dielectric cylinder with normal incidence ($\gamma = 0$) when $2 \leqslant \varepsilon_r \leqslant 6$. The denomination of poles (A_1 , A_2 , B_1 , B_2 , E) is the same as the one of the corresponding irreducible representation of the symmetry group. The zeros of S are conjugated with the poles.

It is interesting to draw the trajectories of the zeros and the poles as a function of the losses in the scatterer. Figure 4 shows them when the imaginary part of the permittivity increases. When the zero trajectories cut the real axis we have a remarkable phenomenon of total absorption for suitable incident fields. Of course, it is not so impressive as for gratings [8], because the total absorption needs a special structure for the incident field (mode structure) not easy to achieve experimentally, but the phenomenon is not different in nature.

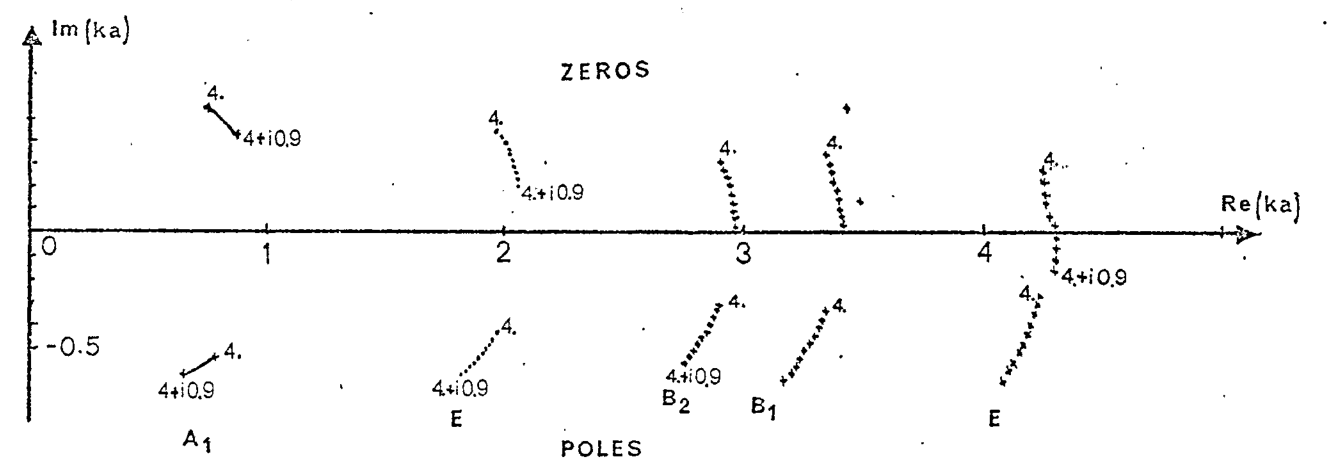

Figure 4

Trajectories of poles and zeros of a square cylinder as a function of the imaginary part of permittivity ($\varepsilon_r = 4. + i\ \varepsilon''$). The incidence is perpendicular to the cylinder axis.

Figure 5 gives the diffraction pattern for a frequency near the cross-over of the real axis and a zero trajectory, for an incident plane wave. Since the plane wave does not have a mode structure, there is some energy diffracted.

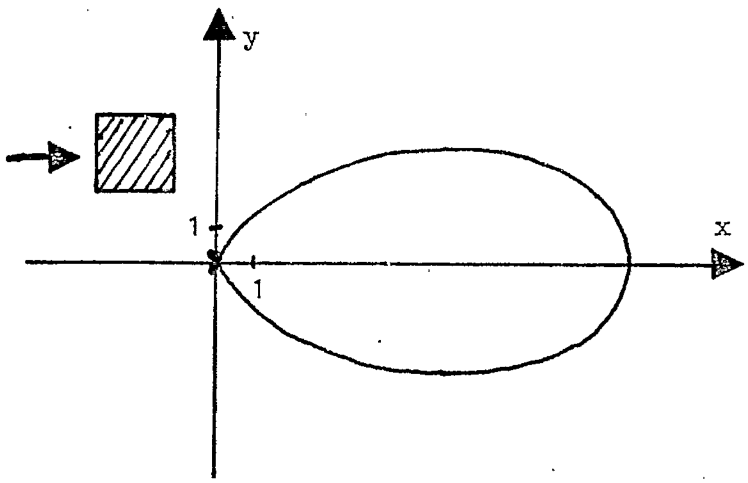

Figure 5

Diffraction pattern of a square cylinder with $\varepsilon_r = 4. + i\ 0.9$ and $ka = 3.4$.

The iterative method used to search the poles needs to know approximate values of them. A raugh localisation could be done by drawing the trajectories in the complex plane of matrix elements as a function of the frequency (figure 6).

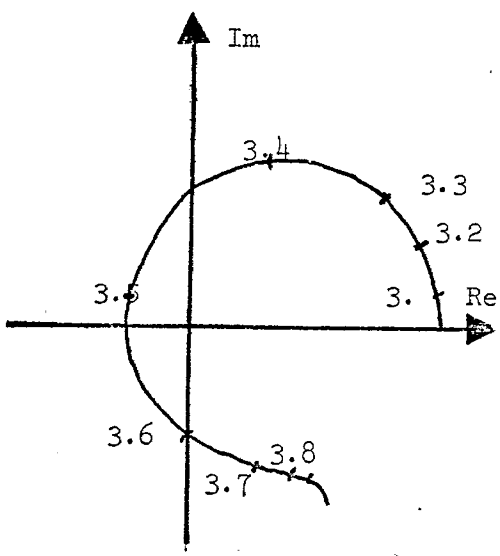

Figure 6-A

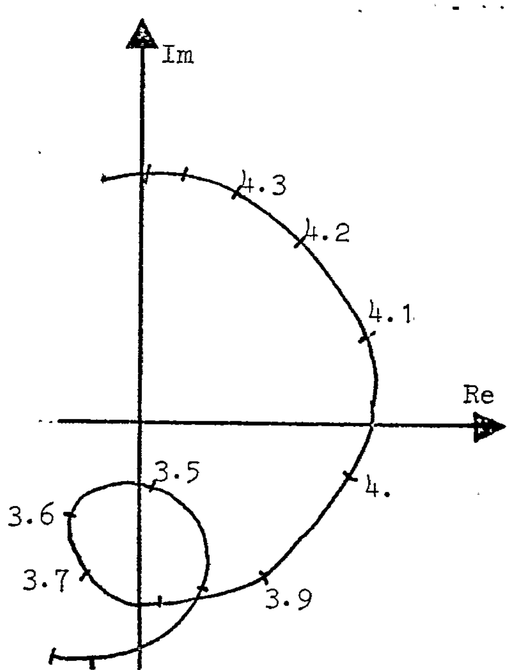

Figure 6-B

Figure 6-A shows the trajectory of a matrix element as a function of the normalized frequency for a detached poles : the argument change is about $3\pi/2$ when passing near the pole.

Figure 6-B shows what happens when two resonances are mixed ; the argument change about 3π if we take the origin inside the loop.

As expected, the pole trajectory on figure 7 tends to the real axis when the projection γ of the wavevector on the cylinder axis increases. The junction point gives the cut-off frequency. The smooth transition shows that it is possible to obtain poles with a small imaginary part even with small permittivity, i.e. to observe sharp resonance peaks.

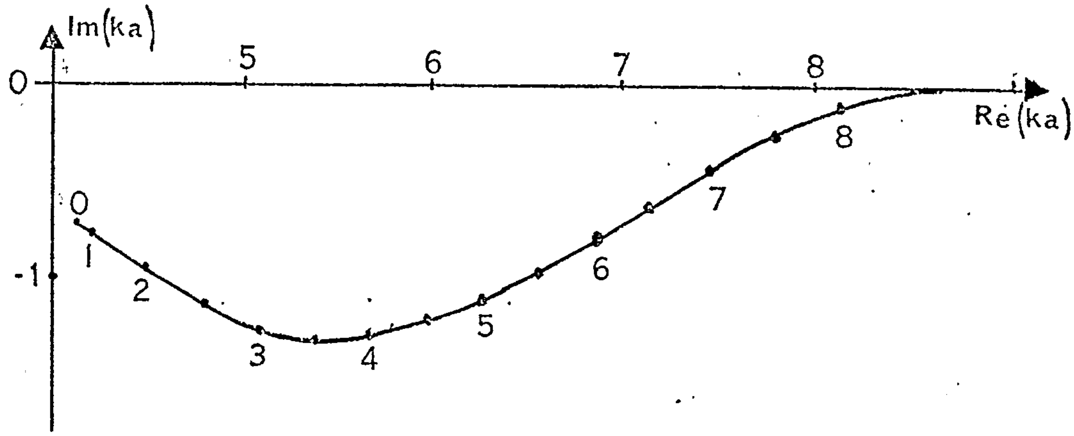

Figure 7

Pole trajectory as a function of the propagation constant γ *.*
The square cylinder has a permittivity $\varepsilon_r = 2.56$ *.*

IV.3. Direct computation of scattering cross sections.

Our program can be also used to draw directly the cross section of a cylinder. Examples are given in figure 8 and figure 9.

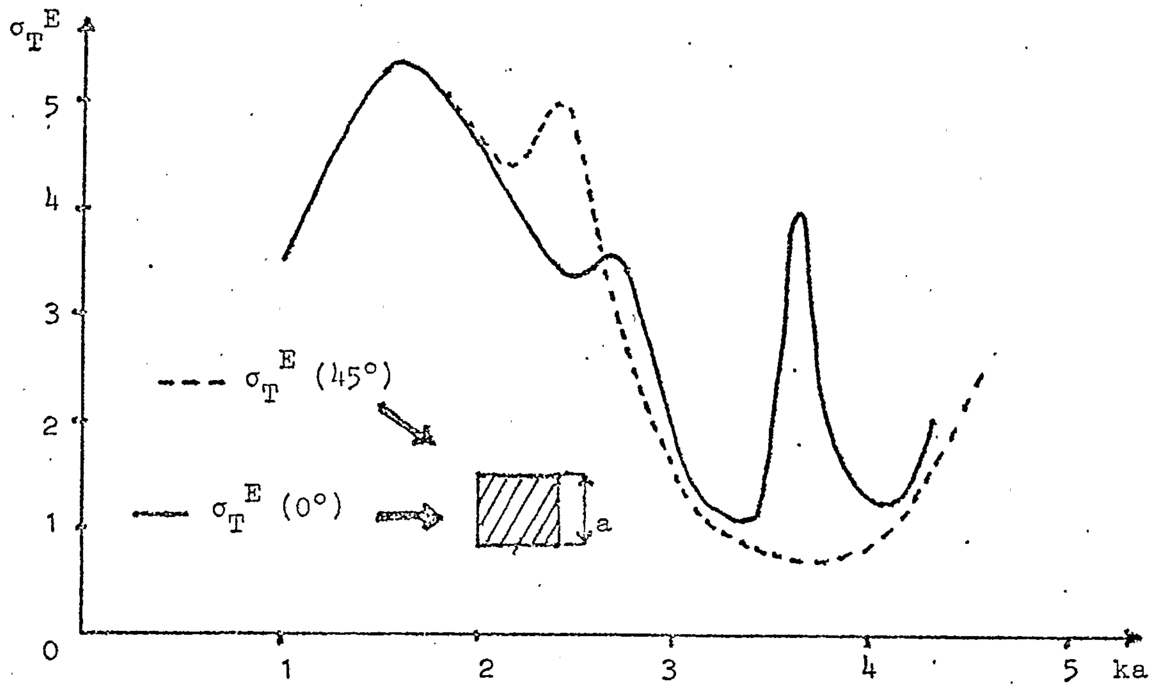

Total cross-section vs. normalized frequency for a square dielectric cylinder ($\varepsilon_r = 6.$), *for two oblique incidences with* $(Oz, \vec{k}) = 45°$, $\vec{k}$ *is the incident wave vector.*

Figure 8

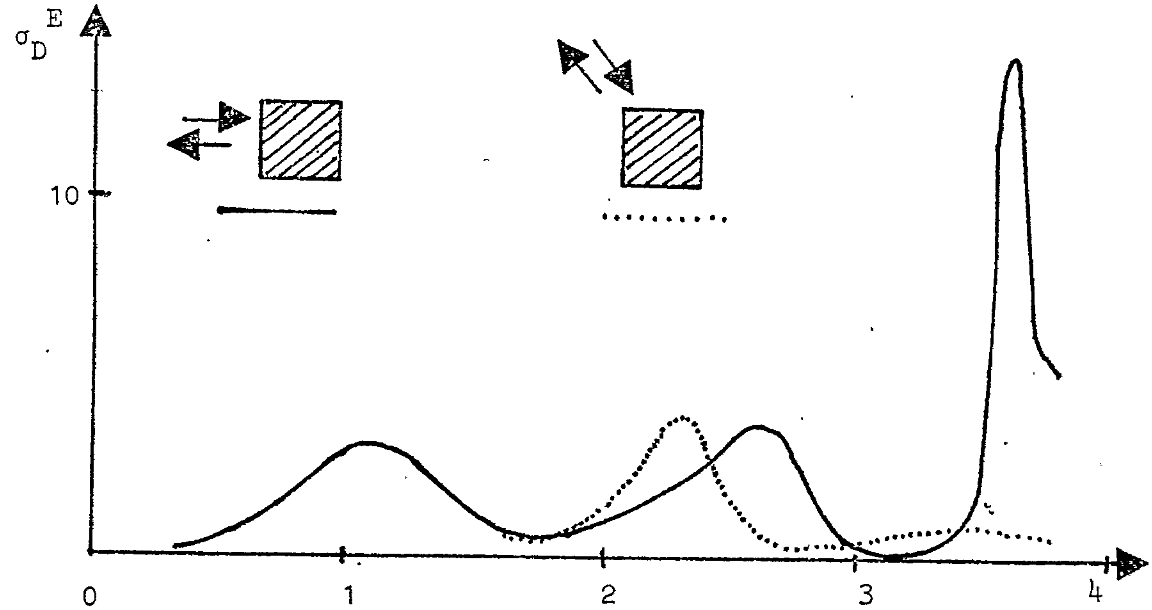

Figure 9

Differential cross-section of a square dielectric cylinder ($\varepsilon_r = 6.$) with $H_z = 0$, $\phi = (\vec{Oz},\vec{k}) = 45°$.

———— $\sigma_D^E(0°,180°)$; - - - - - $\sigma_D^E(45°, 225°)$.

IV.4. Computation of diffraction patterns by the singularity expansion approach.

At a given frequency, the diffraction pattern can be drawn using formula (17). The comparison with directly computed curves gives a good idea about the accuracy of the expansion. An example is given in figure 10.

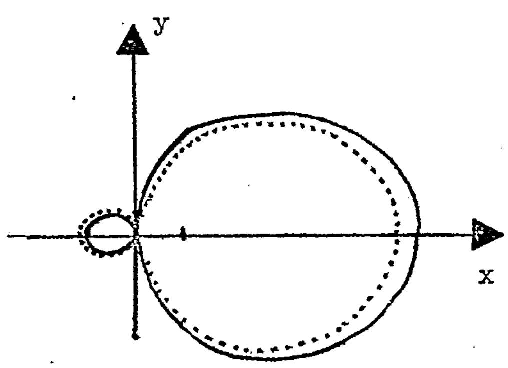

Figure 10-A

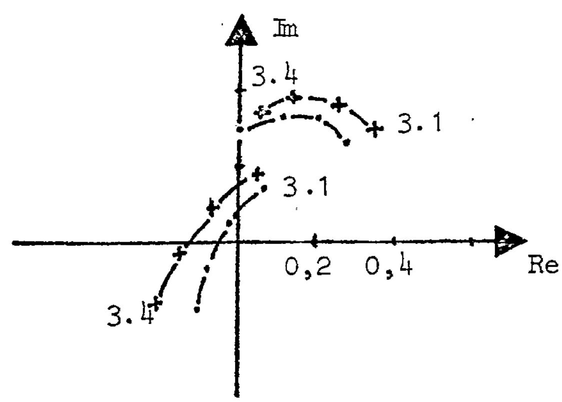

Figure 10-B

Figure 10-A. *Diffraction pattern of a square cylinder ($\varepsilon_r = 6.$) with $H_z = 0$, $\gamma = 0$, $\theta_i = 0$, $ka = 2.5$.*

———— *Direct calculation*
- - - - - *With expansion (17).*

Figure 10-B. *Locus of 2 matrix elements as a function of ka for a square cylinder with losses ($\varepsilon_r = 4. + i\ 0.5$)*

+ — + — *Direct calculation*
· — · — Using formula (17) with the zeros of det(S) instead of k_1 .

V.1. *Introduction.*

We just give briefly the meaning of few words necessary to understand the use of group representation theory in electromagnetic scattering. For further informations, Quantum Mechanic books [24,25], as well as more specialized ones, could be consulted with profit.

Let us define the symmetry group of a scattering object by the set of all the geometrical transformations leaving invariant the object. The number of these transformations is finite because rotations are difined modulo 2π . Thus, it is said that the group is finite.

We take, for example, the symmetry group $\mathcal{G}$ of a square cylinder (fig. 11). It is composed by 8 elements : identity, rotations π , $\pi/2$ and $-\pi/2$ around Oz , plane reflexions with respect to xOz , yOz , and 2 diagonal planes of symmetry.

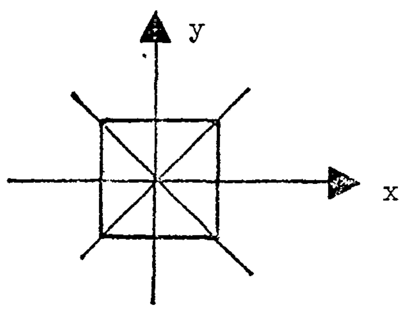

Figure 11

We see that the composition of 2 geometrical transformations of the group gives a new element of the group. Thus, it is possible to draw the group Pythagorean table.

It is important to understand that the group structure is not relevant of the geometrical nature of its transformations. The relations produced by the composition law,between the elements, give the structure : the same "Pythagorean table" can be obtained, starting with 8 square matrices with dimension N . The set of these matrices is said to be a N-dimensional linear representation of the group $\mathcal{G}$. If the matrice multiplication table is deduced from the group table by confounding two or more elements, the representation is said not faithfull.

We use here a set of N $\exp(in\theta)$ basis functions to define the vector space of representation. Height matrices acting into this space will give us the representation itself. Changing the space basis, we get 8 new matrices with the same multiplication table. This new representation of the group is said equivalent to the first one. Practically, we don't distinguish two equivalent representations, and they will have the same denomination. If one can find a basis where all the matrices of the group have the same "diagonal-box" form (figure 12), the represen-

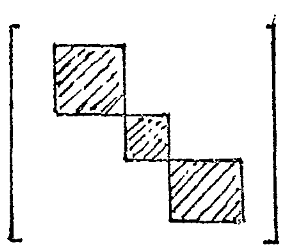

Figure 12

A diagonal box matrix

tation is said decomposed into a direct sum of representations, each corresponding to a "box".

If there is no invariant sub-space with respect to all the transformations of the Group, the representation is irreducible. This notion is very important because it is the foundation of Group theory applications in Physics. For finite groups, it can be shown that all representations could be decomposed in a sum of irreducible representations.

V.2. *Connection between the scattering phenomenon and symmetry group.*

The propagation equations (A-4) are left invariant by the transformation $\mathcal{G}_1$ belonging to the group $\mathcal{G}$. So we can write :

$$\psi^+ = \mathcal{S}\,\psi_0^+ \Longrightarrow \mathcal{G}_1\,\psi^+ = \mathcal{S}\,\mathcal{G}_1\,\psi_0^+ .$$

Consequently :

$$\mathcal{S} = \mathcal{G}_1^{-1}\,\mathcal{S}\,\mathcal{G}_1 \Longrightarrow \mathcal{S} \text{ and } \mathcal{G}_1 \text{ commute : } \left[\mathcal{S}, \mathcal{G}_1\right] = 0 .$$

Let us consider, for example, $\mathcal{S}$ as an operator-valued function of k with pole k_i. We get :

$$\lim_{k\to k_i} (k - k_i)\left[\mathcal{S}, \mathcal{G}_1\right] = 0 .$$

From the definition of residue R_i, we get :

$$\left[R_i , \mathcal{G}_1\right] = 0 .$$

If $|i\rangle$ is an eigenvector of R_i, such as $R_i\,|i\rangle = c_i\,|i\rangle$, we get :

$$R_i\,G_1\,|i\rangle = G_1\,R_i\,|i\rangle = c_i\,G_1\,|i\rangle .$$

Thus $G_1\,|i\rangle$ is also eigenvector of R_i for the same eigenvalue c_i. Consequently, the space defined by the eigenvectors associated with c_i is left invariant by the Group transformations. We assume, as it is done in Quantum Mechanics, that this space defines an irreducible representation and that "the contrary would be an utterly improbable coincidence" [25]. As the group is finite this sub-space may be finite ; this is in accordance with the Fredholm Analytic Theorem [16] for compact operator-valued functions.

We can now associate an irreducible representation $\mathcal{R}_i$ of the symmetry group to each resonance. If $\mathcal{R}_i$ is one-dimensional, the residue R_i is a matrix of rank one and has only one eigenvector $|i\rangle$. This eigenvector is the representation of the resonant mode associated with the residue R_i. If the dimension of $\mathcal{R}_i$ is greater than one, R_i has independent eigenvectors, and a resonant mode corresponds to any linear combination of eigenvectors : it is a degenerated resonance.

The same properties also holds for $\mathcal{S}$ as a function of propagation constant γ . Consequently each waveguide mode is associated to an irreducible representation of the symmetry group cross section. We think that it gives a logical way to designate the modes.

V.3. The characterization of représentations.

The diagonal elements sum (i.e. the trace) of a matrix G_1 representing one element of the group $\mathcal{G}$ remains the same in a change of basis : it is called its character. Thus, two equivalent representations have the same characters.

Two elements of a group having the same characters for all possible inequivalent irreducible representations are of the same class. It can be shown that the number of classes is equal to the number of irreducible representations of a group.

The square cylinder has five inequivalent irreducible representations [25] noted A_1 , A_2 , B_1 , B_2 and E . The five classes are :

E_i for the identity I ,

C_2 " rotation $R(\pi)$,

$2C_4$ " rotations $R(\pi/2)$ and $R(-\pi/2)$,

2σ " plane reflexions with respect to xOz : σ/xOz or yOz : σ/yOz,

$2\sigma'$ " " " with respect to the diagonals.

The table of characters is given in table 2.

C_{4v}	E_i	C_2	$2C_4$	2σ	$2\sigma'$
A_1	1	1	1	1	1
A_2	1	1	1	-1	-1
B_1	1	1	-1	1	-1
B_2	1	1	-1	-1	1
E	2	-2	0	0	0

Table 2

The table of characters for the symmetry group C_{4v} of a square cylinder (C_{4v} is isomorph to group D_4 used in theoretical physics)

The dimensions of representations are equal to the character of E_i . We see that A_1 , A_2 , B_1 , B_2 are one-dimensional representations and E a two-dimensional one.

Practically, for a given resonance, we compute the eigenvector on the exp(inθ) basis. It is the Fourier expansion of a function $u(\theta)$.

Performing one transformation of the group is equivalent to change θ into θ'. Thus, we get 8 functions and comparing these functions to the initial one, we determine the characters of the representation attached to the resonance. Using the table 2, we get the corresponding irreducible representation. This procedure allows us to classify logicaly the resonances of the cylinder with respect to their symmetry properties, whatever the shape of the scatterer is.

V.4. *The interest of a logical mode denomination.*

A good example of the disadvantages of the traditional mode denomination for square waveguides is given by Stalzer et al. in a recent paper [26]. They show that in a square waveguide made with a perfect conductor, modes TE_{02} and TE_{20} are degenerated. If the section is a cross such as the one represented in figure 13, the degeneracy is broken. On the contrary, TE_{01} and TE_{10} modes remain degenerate. Thus, the usual mode denomination does not allow us to predict this phenomenon. But the symmetry properties of TE_{01} and TE_{10} show that these modes are connected to a bi-dimensional irreducible representation E . Thus, TE_{01} and TE_{10} remain degenerate for all cross-sections having the same symmetry group C_{4v} . The phenomenon is different for TE_{20} and TE_{02} . The symmetry properties show that the sum $TE_{02} + TE_{20}$ has the symmetries of an A_2 irreducible representation, and that the difference $TE_{02} - TE_{20}$ has the symmetries of a B_2 one. Thus, we can say that the degeneracy of TE_{02} and TE_{20} is an hazard caused by the infinite conductivity of the waveguide walls for a square cross section. Thus, the degeneracy is removed when the cross-section has the same symmetry group but is not a square.

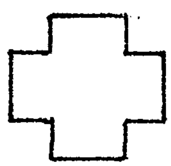

Figure 13

Guide cross-section with symmetry Group C_{4v}

V.5. *Selection rules for one-dimensional representations.*

The interest of the classification of resonances is not purely formal : it is the first step to found selection rules for differential cross-section. These rules are consequences of the following theorem [25] : Let $\mathfrak{C}$ be an operator invariant with respect to all symmetry transformation, $|i\rangle$ and $|j\rangle$ the vectors of 2 spaces of irreducible (non-unit) representations. The matrix elements :

$$\langle j| \mathfrak{C} |i\rangle$$

are zero if $|i\rangle$ and $|j\rangle$ are related to inequivalent irreducible representations.

V.5.1. *Selection rules for diffracted directions.*

Let us consider an incident field ψ^- with frequency close to a natural frequency resonance ($k \# \mathrm{Re}(k_i)$). The main contribution to diffracted field generally comes from the residue R_i , corresponding to the resonant mode excited by the sources. Thus, the diffraction pattern is essentially a picture of a resonant mode.

For the sake of simplicity, let us assume that the incident field propagates normaly to Oz with the electric field $\vec{E}^i$ parallel to Oz †. Thus, the differential cross-section is [10] :

$$(18) \qquad \sigma_B = \lim_{r\to\infty} 2\pi r \frac{|\vec{E}^s|^2}{|\vec{E}^i|^2} = 2\pi \, |\mathcal{E} \, \psi_0^+|^2 .$$

We write $|i\rangle$ for ψ_0^+ and $|d\rangle$ for Dirac distribution $\delta(\theta - \theta_d)$. We get :

$$(19) \qquad \sigma_B = 2\pi \, |\langle d| \, \mathcal{E} \, |i\rangle|^2 .$$

Near the resonance, there is only the residue R_i contributing to $\mathcal{E}|i\rangle$, and we can assume that $|i\rangle$ belongs to the irreducible representation $\mathcal{R}_i$ attached to the pole. Changing $\theta - \theta_d$ into $-(\theta - \theta_d)$ leaves $\delta(\theta - \theta_d)$ invariant : we define the group of symmetry $\mathcal{G}_d$ of $|d\rangle$ by the two elements : identity and plane-reflexion with respect to the direction of diffraction θ_d . We find the group C_s , whose table of characters is given in table 3.

$C_s(\theta_d)$	E_i	σ_d
A	1	1
B	1	-1

E_i is the identity

σ_d is the plane symmetry with respect to the plane $(Oz,\vec{u})$ with $(\vec{Ox},\vec{u}) = \theta_d$

Table 3

An interesting case arises when C_s is a subgroup of the group $\mathcal{G}$ of the scatterer. For a square cylinder, it occurs when the direction of diffraction is parallel to an axis or a bissectrix ($\sigma_d = \sigma$ or $\sigma_d = \sigma'$). Of course $|d\rangle$ belongs to the representation A of C_s ($|d\rangle$ is symmetric with respect to σ).

Let us consider an irreducible one-dimensional representation $\mathcal{R}_i$ of $\mathcal{G}$. It is also an irreducible representation of $\mathcal{G}_d$. If we take the two elements of $\mathcal{G}$ existing in $\mathcal{G}_d$, we get the characters of a given representation.

For example, if $\mathcal{G} = C_{4v}$, the characters of a B_2 representation are :

..../.

† This restriction permits to ignore the complexity introduced by intrinsic symmetry of the field. Here, this symmetry shows itself by the pseudovector nature of H_z , and implies different relations between vector components H_n .

C_{4v}	E_i	C_2	$2C_4$	2σ	$2\sigma'$
B_2	1	1	−1	−1	1

If $\sigma_d = \sigma$, we extract for $\mathcal{G}_d = C_s$:

C_s	E_i	$\sigma_d = \sigma$
B_2	1	−1

By identification with table 3 , we conclude that B_2 of C_{4v} is also a representation $\dot{B}$ of C_s : it is antisymmetric with respect to axis Ox or Oy . Consequently the field diffracted towards these two directions is null, as shown in figure 14.

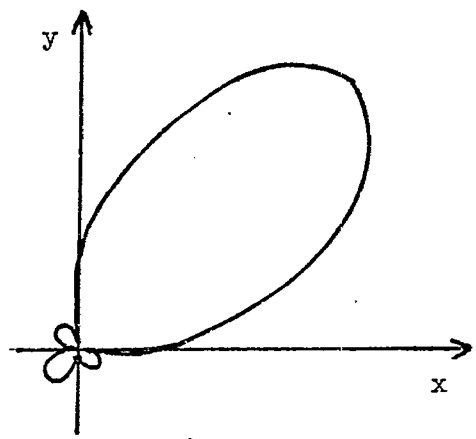

Figure 14

$\sigma(45°, \theta_d)$ for a B_2 resonance at $ka = 2.5$

In other words, the table of characters gives us informations about the symmetry or antisymmetry of a mode with respect to particular directions.

V.5.2. Selection rules for the excitation of modes.

Of course the same theorem could be used when the incident field ψ_0 has particular symmetries. Our case of interest will be a plane wave : it has the same symmetry as $\delta(\theta - \theta_d)$. Consequently, we see that, according to the reciprocity theorem, a resonance cannot be excited by a plane wave propagating in a direction where the resonance does not radiate. This can be seen by comparing figure 15-A and 15-B.

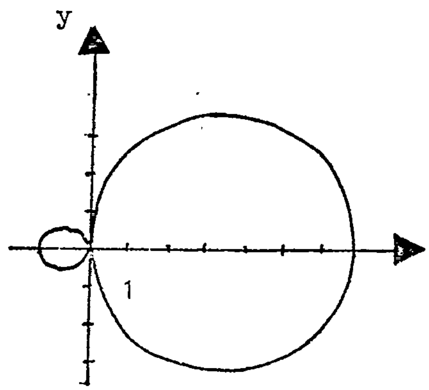

Figure 15-A

$ka = 2.5$

$\sigma_d(0°, \theta_d)$: *the resonance* B_1 *is only excitated*

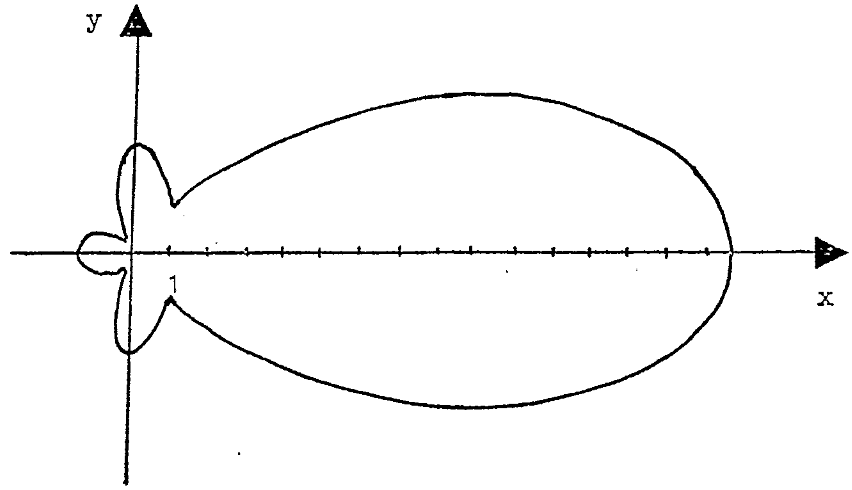

Figure 15-B

$ka = 2.8$

$\sigma_d(0°, \theta_d)$: *the resonance* B_1 *is only excitated*

V.6. *Selection-rules for degenerated resonances.*

When the resonance is degenerated, the corresponding irreducible representation of $\mathcal{G}$ is multi-dimensional. Thus, it is not an irreducible representation of C_s and it must be decomposed. The following relation is convenient to achieve this decomposition :

$$(20) \qquad n = \frac{1}{g} \sum_{\mathcal{G}} \mathrm{trace}(G_i)\, \overline{\mathrm{trace}(G_i^!)} \quad ,$$

n is the number of irreducible representation R of $\mathcal{G}_d$ in the decomposition,

g is the number of elements in $\mathcal{G}_d$,

$\mathrm{trace}(G_i)$ is the character of element G_i of the group $\mathcal{G}$ we want to decompose,

$\mathrm{trace}(G_i^!)$ is the character to the corresponding element of the representation $\mathcal{R}$ of $\mathcal{G}$.

For example the irreducible representation E of C_{4v} can be decomposed into irreducible representations of C_s (elements : E_i and σ/Ox) by :

Decomposition on A of C_s :

$$n = \frac{1}{2}\,(2\times 1 + 0\times 1) = 1 \;.$$

Decomposition on B of C_s :

$$n = \frac{1}{2}\,(2\times 1 + 0\times 1) = 1 \;.$$

$\Longrightarrow$ Each irreducible representation of C_s appears one time in the decomposition. It is the same for the other planes of symmetry σ . Consequently, the E resonances are always excited by a plane wave of suitable frequency, and here no selection rule holds.

But, for given directions of incidence and diffraction, we can find selection rules. The incident field excites only one particular linear combination of degenerate modes, and imposes additional symmetries. For example, a direction of incidence $\theta_i = 0$ implies a plane symmetry with respect to xOz . As −2 is the character of the rotation $R(\pi)$ in the bidimensional representation E (table 2), the corresponding diagonal matrix is $\begin{bmatrix} -1 & 0 \\ 0 & -1 \end{bmatrix}$ and all the linear combinations are anti-symmetric with respect to Oz. Putting together this anti-symmetry and the symmetry with respect to Ox , we conclude that the excitated mode is anti-symmetric with respect to Oy . Consequently no energy is diffracted in the Oy direction. This can be seen in figure 16.

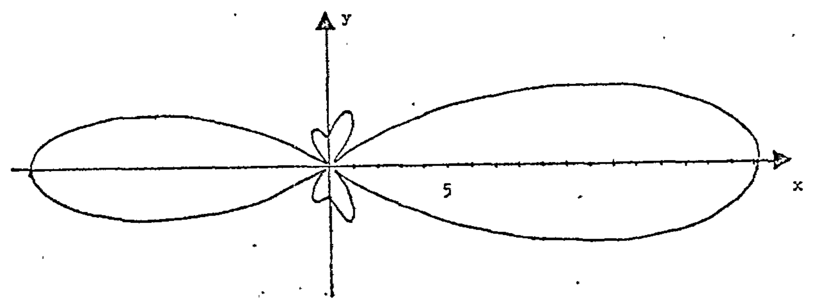

Figure 16

$\sigma(0,\theta)$ for $ka = 3.5$. The resonance E does not radiate in a direction perpendicular to incident wave.

This is an example of selection rules occurring in multi-dimensional resonances.

V.7. *The splitting of degenerate resonances*.

Group theory allows us to know if a degenerate resonance is splitted or remain degenerate when the scatterer loses a part of its symmetries.

Let us continue with our square cylinder for example. If we transform the square into a rectangle, what will happen to E-type degenerate resonance ? Formula (20) gives the answer. The symmetry group of a rectangular-cylinder is C_{2v} . Its characters are given in table 4.

C_{2v}	E_i	C_2	σ_{Ox}	σ_{Oy}
A_1	1	1	1	1
A_2	1	1	−1	−1
B_1	1	−1	1	−1
B_2	1	−1	−1	1

Table 4

The table of characters of C_{2v}

Formula (20) shows that E representations of C_{4v} are decomposed in two inequivalent representations (B_1 and B_2) of C_{2v}. Thus, outside an "utterly improbable coïncidence", going from square to rectangular cylinders, E resonances are splitted into two different parts, occuring for different frequencies. Selection rules show that one part is excitated by a plane wave propagating along Ox (this corresponds to the part B_1 of C_{2v}) and the other, by an incident wave propagating along Oy (part B_2 of C_{2v}). This is illustrated in figure 17, giving the back scattering cross-section of a rectangular cylinder for these two incidences. The resonance which occurs for ka = 3.4 gives two maxima for different values of ka ; this is not the case for the A_1 resonance corresponding to ka = 4.

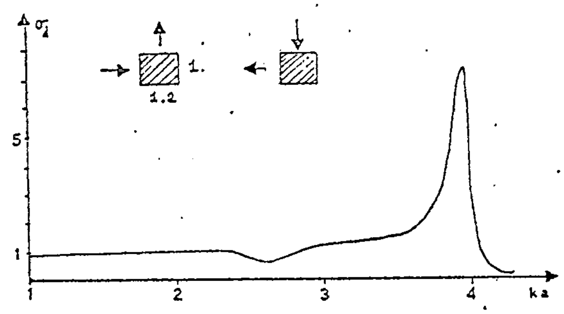

Figure 17-A

Back scattering cross-section for a rectangular cylinder ($\varepsilon_r = 6.$, $H_z = 0$, $\gamma = 0$)

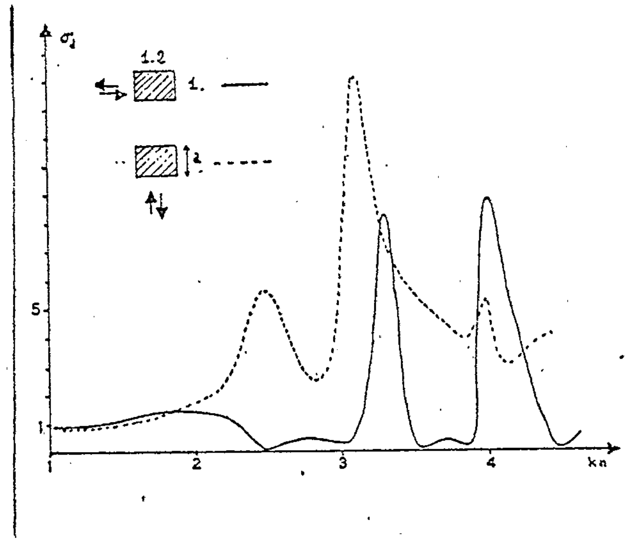

Figure 17-B

Transverse scattering : the reciprocity theorem implies that the two curves are superposed

When the direction of diffraction is perpendicular to the incident one, the reciprocity theorem imposes that the curves are the same for the two incidences. Consequently, as shown in figure 17-B, only non degenerate resonances hold here.

V.8. Separated and mixed resonances.

From the preceding considerations, we see that two resonances relevant from inequivalent irreducible representations can be said separated : even if the corresponding poles lies near each other in the complex plane, formula (17) is valid. This is not obvious on scattering cross-section curves, because resonance peaks are then superposed. On the contrary, two poles connected with equivalent irreducible representations gives mixed resonances, and necessitate a more elaborated formula than (17). Consequences on matrix elements are shown in figure 6-B.

V.9. *Conclusion and perspectives*.

As we have tried to show here, the scattering operator singularities contain numerous informations about the diffraction of electromagnetic waves by a cylinder. These informations allow not only an efficient calculation of the diffracted field, but also give a better understanding of the phenomenon. We think that, in this case, this method is a substantial improvement compared to the diagonalization of operators upon the real axis which gives the characteristic modes [27].

We deal here with cylinders of finite cross-section such as dielectric rods, but diffraction operators may also be determined for other scatterer [28,29]. The differential formalism proposed here is now transposed to cylinders with infinite periodic cross-section such as gratings, grating-couplers and DFB Lasers. A program has began to work and gives a good agreement with measurements. We hope to be able to give more details about this new development in a next paper.

References

[1] C.E. Baum, "On the singularity expansion method for the solution of electromagnetic interaction problems", Interaction note 88, Déc. 1971.

[2] C.E. Baum, "The singularity expansion method", Topics in Applied Physics Transient Electromagentic Fields, (L.B. Felsen editor) 1976, Springer-Verlag, (Berlin, New-York), p. 129-179.

[3] L. Marin, "Natural-Mode representation of transient scattered fields", IEEE Trans. Ant. Prop., Vol. AP-21, n° 6, Nov. 1973.

[4] L.Pearson, R. Mittra, "Causality considerations in SEM coupling coefficients forms", Proc. AP-S International Symposium (Oct. 1976), Session 16-B, p. 528-531.

[5] F.M. Tesche, "On the analysis of scattering and Antenna problems using the singularity expansion technique", IEEE Trans. Ant. and Prop. (USA), Vol. AP-21, n° 1, Janvier 1973, p. 53-62.

[6] R.J. Garbacz, R.H. Turpin, "A generalized expansion for radiated and scattered fields", IEEE Trans. AP-19, N° 3, May 1971, p. 348-358.

[7] M. Nevière, P. Vincent, R. Petit and M. Cadilhac, "Determination of the coupling coefficient of a holographic thin film coupler", Optics Commun;, Vol. 9, n° 3, (Nov. 1973), p. 240-245.

[8] D. Maystre and R. Petit, "Brewster incidence for metallic grating", Optics Commun., 17, n° 2, 1976, p. 196-200.

[10] P. Vincent, M. Nevière, "Matrice de diffraction et fréquences naturelles de résonance d'un cylindre", Ann. des Télécom. 31, n° 3-4, Mars-Avril 1976.

[9] M. Nevière, D. Maystre, P. Vincent, "Application du calcul des modes de propagation à l'étude théorique des anomalies des réseaux recouverts de diélectrique", Nouv. Rev. Opt., accepted for publication.

[11] J. Van Bladel, "Electromagnetic fields", Mc Graw-Hill Book Co. (New-York, London), USA (1964), p. 250.

[12] P. Roman, "Advanced quantum theory", Addison-Wesley Publishing Cy., Reading (Mass.) USA, 1965.

[13] A.C. Hewson, "An introduction to the theory of electromagnetic waves, Longman Group Ltd, London (1970).

[14] A.T. de Hoop, "A reciprocity theorem for the electromagnetic field scattered by an obstacle", Appl. Sci. Res., Sect. B, 8 , p. 135-139, 1960.

[15] J.A. Stratton, "Electromagnetic theory", New-York, Mc Graw-Hill, 1941.

[16] M. Reed, B. Simon, "Methods of modern mathematical physics". Tome I : Functional analysis. Academic Press, New-York and London, 1972.

[17] J.R. Wait, "Advances in radio research", (J.A. Saxton editor), Vol. 1, p. 157-217, Academic-Press, New-York and London, 1964.

[18] W. Franz and P. Beckmann, IRE Trans. Ant. Prop., AP-4, 203 (1956).

[19] J.P. Hugonin, R. Petit, "A numerical study of the problem of diffraction at a non-periodic obstacle", Optics Commun., Vol. 20, n° 3 (Mars 1977), p. 360-364.

[20] A.C. Lind, J.M. Greenberg, "Electromagnetic scattering by obliquely oriented cylinders", J. Applied Physics, 37, n° 8, (July 1966), p. 3195.

[21] P. Vincent, D. Maystre et R. Petit, "Determination and analysis of diffraction patterns for a cylindrical obstacle in the resonance region", Proc. 5th Col. on Microwave Communication, Budapest (24-30 Juin 1974), vol. ET, p. 405-413.

[22] D. Maystre et P. Vincent, "Diffraction d'une onde électromagnētique plane par un objet cylindrique non infiniment conducteur de section arbitraire", Optics Comm., 1972, Vol. 5, n° 5, p. 327-330.

[23] J.Goell, "A circular-harmonic computer analysis of rectangular-dielectric waveguides", Bell Syst. J., Vol. 48, 2133 (1969).

[24] A. Messiah, "Mecanique Quantique", Dunod (Paris), t. 2.

[25] Landau et Lifchitz, "Quantum Mechanics", Pergamon Press (Paris).

[26] J.H. Stalzer, M.D. Greenman and F.G. Willewerth, "Modes of crossed rectangular waveguide", IEEE Trans. AP-24, n° 2 (March 1976), p. 220-223.

[27] R.F. Harrington, "Characteristic modes for antennas and scatterers", "Numerical and assymptotic techniques in electromagnetics", (R. Mittra editor), p. 51-87. Springer Verlag (Berlin, Heidelberg, New York), 1975.

[28] A. Saad, H.L. Bertoni and T. Tamir, "Beam scattering by non-uniform leaky-wave structure", Proc. IEEE, Vol. 62, n° 11 (Nov. 1974), p. 1552-1561.

[29] M. Nevière et P. Vincent, "Sur une propriété de symétrie des réseaux diélectriques", Optica Acta, 1976, Vol. 23, n° 7, p. 557-568.

ANNEX A

The electromagnetic field verifies Maxwell equations :

$$\vec{\nabla} \times \vec{E} = -\mu \frac{\partial \vec{H}}{\partial t}$$

$$\vec{\nabla} \times \vec{H} = \varepsilon \frac{\partial \vec{E}}{\partial t}$$

Using (2) and projecting on Oz and xOy , we get :

$$\text{(A-1)} \quad \begin{cases} \vec{\nabla} \times \vec{E}_T = i\,\omega\,\mu\,H_z\,\vec{e}_z \\ \vec{\nabla} \times \vec{H}_T = -i\,\omega\,\varepsilon\,E_z\,\vec{e}_z \end{cases}$$

$$\text{(A-2)} \quad \begin{cases} \vec{\nabla}\,E_z \times \vec{e}_z + i\,\gamma\,\vec{e}_z \times \vec{E}_T = i\,\mu\,\omega\,\vec{H}_T \\ \vec{\nabla}\,H_z \times \vec{e}_z + i\,\gamma\,\vec{e}_z \times \vec{H}_T = -i\,\omega\,\varepsilon\,\vec{E}_T \end{cases}$$

with $\tilde{k}^2 = \omega^2 \varepsilon \mu - \gamma^2$, we have [13] :

$$\text{(A-3)} \quad \begin{cases} \vec{E}_T = \dfrac{1}{\tilde{k}^2} \left(-i\,\omega\,\mu\,\vec{e}_z \times \vec{\nabla}\,H_z + i\,\gamma\,\vec{\nabla}\,E_z\right) \\[2ex] \vec{H}_T = \dfrac{1}{\tilde{k}^2} \left(i\,\omega\,\varepsilon\,\vec{e}_z \times \vec{\nabla}\,E_z + i\,\gamma\,\vec{\nabla}\,H_z\right) . \end{cases}$$

From (A-2) we get the propagation equations. As all the differential operators act on continuous quantities, these equations are true in the sense of distributions as well as in the sense of functions :

$$\text{(A-4)} \quad \begin{cases} \vec{\nabla} \times \left[\dfrac{\varepsilon}{\tilde{k}^2}\,\vec{e}_z \times \vec{\nabla}\,E_z + \dfrac{\gamma}{\omega\,\tilde{k}^2}\,\vec{\nabla}\,H_z\right] + \varepsilon\,E_z\,\vec{e}_z = 0 \\[2ex] \vec{\nabla} \times \left[\dfrac{-\mu}{\tilde{k}^2}\,\vec{e}_z \times \vec{\nabla}\,H_z + \dfrac{\gamma}{\omega\,\tilde{k}^2}\,\vec{\nabla}\,E_z\right] - \mu\,H_z\,\vec{e}_z = 0 . \end{cases}$$

With $\varepsilon = \varepsilon_r\,\varepsilon_0$, $\mu = \mu_0$, and ∂_r being the partial derivative with respect to r , we get :

$$\text{(A-5)} \quad \boxed{\begin{aligned} &\partial_r \left[\frac{r\,\varepsilon_r}{\tilde{k}^2}\,\partial_r E_z + \frac{\gamma}{\omega\,\varepsilon_0\,\tilde{k}^2}\,\partial_\theta H_z\right] - \partial_\theta \left[\frac{-\varepsilon_r}{r\,\tilde{k}^2}\,\partial_\theta E_z + \frac{\gamma}{\omega\,\varepsilon_0\,\tilde{k}^2}\,\partial_r H_z\right] + r\,\varepsilon_r\,E_z = 0 \\ &\partial_r \left[\frac{-r}{\tilde{k}^2}\,\partial_r H_z + \frac{\gamma}{\omega\,\mu_0\,\tilde{k}^2}\,\partial_\theta E_z\right] - \partial_\theta \left[\frac{1}{r\,\tilde{k}^2}\,\partial_\theta H_z + \frac{\gamma}{\omega\,\mu_0\,\tilde{k}^2}\,\partial_r E_z\right] - r\,H_z = 0 . \end{aligned}}$$

ANNEX B

A reciprocity theorem.

We start from a well known relation of reciprocity for isotrope medium [11] :

$$\iint_{\mathcal{C}_2} (\vec{E} \times \vec{H}') \cdot \vec{n}\, dS = \iint_{\mathcal{C}_2} (\vec{E}' \times \vec{H}) \cdot \vec{n}\, dS , \tag{B-1}$$

$(\vec{E},\vec{H})$ and $(\vec{E}',\vec{H}')$ are two given fields satisfying Maxwell equations, $\mathcal{C}_2$ is the circular cylinder of axis Oz and radius R_2 .

The field $(\vec{E},\vec{H})$ has an outgoing part $(\vec{E}^+,\vec{H}^+)$; we define :

$$\vec{E}^+(r,\theta,z,t) = \mathrm{Re}\left[\vec{E}(\theta)\ \phi(r,z)\ \exp(-i\omega t)\right] .$$

From Maxwell equations, for $r > R_2$, we get :

$$\vec{\nabla} \cdot \vec{E}^+ = 0 \Longrightarrow \phi(r,z)\ \vec{\nabla}\, \vec{E}(\theta) + \vec{\nabla}\, \phi(r,z) \cdot \vec{E}(\theta) = 0 . \tag{B-2}$$

When r tends to infinity : $\vec{\nabla}\, \vec{E}(\theta) \sim \frac{1}{r}\, \partial_\theta\, E_\theta(\theta) = 0\left(\frac{1}{\sqrt{r}}\right)$ and from (3) :

$$\phi(r,z) \sim \exp\left[i(\gamma z + \tilde{k}_0 r)\right] r^{-1/2} .$$

Using (B-2), we conclude that $\vec{\nabla}\, \phi(r,z)$ is perpendicular to $\vec{E}(\theta)$.

Also $r \to \infty \Longrightarrow \vec{\nabla}\, \phi(r,z) \sim i\ (\tilde{k}_0 \vec{n} + \gamma\ \vec{e}_z)\ \phi(r,z)$.

As $\tilde{k}_0$ is the projection of $\vec{k}_0$ upon the xOy plane and γ its projection on the Oz axis, we have shown that the diffracted electric field is perpendicular to its direction of propagation $\vec{k}_0$.

The Maxwell equation :

$r > R_2$: $\vec{\nabla} \times \vec{E}^+ = -\, i\ \omega\ \mu_0\ \vec{H}^+$ gives :

$$r \to \infty : \quad \vec{H}^+ \sim \frac{i}{\omega\ \mu_0}\, \vec{\nabla}\, \phi(r,z) \times \vec{E}(\theta) \sim \frac{\vec{k}_0}{\omega \mu_0} \times \vec{E}(\theta)\ \phi(r,z) = \frac{\vec{k}_0 \times \vec{E}^+}{k_0\ Z_0} . \tag{B-3}$$

Far from the cylinder, the diffracted field has locally the same structure as a plane wave propagating with an angle $\varphi = (Oz,\vec{k}_0)$.

This implies that providing that the incoming fields propagate with the same angle φ , **for** $R_2 \to \infty$:

$$\iint_{\mathcal{C}_2} (\vec{E}^+ \times \vec{H}'^+) \cdot \vec{n}\, dS = \iint_{\mathcal{C}_2} (\vec{E}'^+ \times \vec{H}) \cdot \vec{n}\, dS . \tag{B-4}$$

The incoming part always satisfies Maxwell equations with $\varepsilon = \varepsilon_0$, $\mu = \mu_0$, thus we get :

$$\iint_{\mathcal{C}_2} (\vec{E}^- \times \vec{H}'^-) \cdot \vec{n}\, dS = \iint_{\mathcal{C}_2} (\vec{E}'^- \times \vec{H}^-) \cdot \vec{n}\, dS . \tag{B-5}$$

From (B-4), (B-5) and (B-1), we get :

$$R_2 \to \infty : \iint_{\mathcal{C}_2} (\vec{E}^- \times \vec{H}'^+ + \vec{E}^+ \times \vec{H}'^-)\vec{n}\, dS = \iint_{\mathcal{C}_2} (\vec{E}'^- \times \vec{H}^+ + \vec{E}'^+ \times \vec{H}^-)\vec{n}\, dS . \tag{B-6}$$

From (A-5), it can be shown without difficulties that :

$$R_2 \to \infty : \quad \iint_{\mathcal{C}_2} (\vec{E} \times \vec{H}')\vec{n}\, dS \sim \frac{-i\omega\varepsilon_0}{\tilde{k}_0{}^2} \iint_{\mathcal{C}_2} E_z\, \partial_r\, E'_z\, dS - \frac{i\omega\mu_0}{\tilde{k}_0{}^2} \iint_{\mathcal{C}_2} H'_z\, \partial_r\, H_z\, dS. \quad \text{(B-7)}$$

From (B-6) and (B-7), a tedious but elementary calculation shows that :

$$S_{m,p}^{n,q} = S_{-n,q}^{-m,p}$$

A N N E X C

Computation of the S-matrix.

We use the same method as in [21]. Let us consider that ε and μ are constants for $r < R_1$ and $r > R_2$. We use expansion (3) in Hankel function if $r > R_2$, and similar expansion with Bessel functions if $r < R_1$. The S-matrix gives the coefficients of the outgoing waves in expansion (3) from the coefficients of the incoming waves. Of course, we only compute a finite matrix of N order. We begin by taking N arbitrary linearly independent values for the field in $r = R_1$; N simultaneous integrations by Runge-Kutta algorithm give N values for the field and its normal derivative on $r = R_2$. Suitables linear combinations give the corresponding outgoing and incoming waves, which can be written in terms of matrices M_+ and M_-. Then the S-matrix is obtained by : $S = M_+ (M_-)^{-1}$.

We must take care to use integration algorithm with continuous functions with respect to r. This can be done if we write propagation equations (A-5) as a differential system of the first order. We define :

$$\tilde{E} = \frac{\varepsilon_r r}{\tilde{k}^2} \partial_r E_z + \frac{\gamma}{\omega \varepsilon_0} \frac{1}{\tilde{k}^2} \partial_\theta H_z ,$$

$$\tilde{H} = \frac{-r}{\tilde{k}^2} \partial_r H_z + \frac{\gamma}{\omega \mu_0} \frac{1}{\tilde{k}^2} \partial_\theta E_z ,$$

and we get :

$$\left\{ \begin{aligned} \partial_r E_z &= \frac{-\gamma}{\omega \varepsilon_0 \varepsilon_r} \frac{1}{r} \partial_\theta H_z + \frac{\tilde{k}^2}{r \varepsilon_r} \tilde{E} , \\ \partial_r H_z &= \frac{\gamma}{\omega \mu_0 r} \partial_r E_z - \frac{\tilde{k}^2}{r} \tilde{H} , \\ \partial_r \tilde{E} &= \partial_\theta \left[\frac{-1}{\omega^2 \varepsilon_0 \mu_0} \frac{1}{r} \partial_\theta E_z - \frac{\gamma}{\omega \varepsilon_0 r} \tilde{H} \right] - r \varepsilon_r E_z , \\ \partial_r \tilde{H} &= \partial_\theta \left[\frac{1}{\omega^2 \varepsilon_0 \mu_0} \frac{1}{r} \partial_\theta H_z + \frac{\gamma}{\omega \mu_0 \varepsilon_r} \frac{1}{r} \tilde{E} \right] + r H_z . \end{aligned} \right.$$

Using the $\exp(in\theta)$ Fourier basis, we have a set of ordinary coupled differential equations. If we call E_n the n th component of E_z, we get :

$$\left\{ \begin{aligned} \frac{dE_n}{dr} &= \frac{-i\gamma}{\omega \varepsilon_0} \frac{1}{r} \sum_m m \, (\varepsilon^{-1})_{n-m} H_m + \frac{1}{r} \sum_m \left(\frac{\tilde{k}^2}{\varepsilon_r} \right)_{n-m} \tilde{E}_m \\ \frac{dH_n}{dr} &= \frac{i\gamma}{\omega \mu_0} \frac{1}{r} n E_n - \frac{1}{r} \sum_m (\tilde{k}^2)_{n-m} \tilde{H}_m \\ \frac{d\tilde{E}_n}{dr} &= \frac{n^2}{k_0^2} \frac{1}{r} E_n - \frac{i\gamma}{\omega \varepsilon_0} \frac{1}{r} n \tilde{H}_n - r \sum_m (\varepsilon_r)_{n-m} E_m \\ \frac{d\tilde{H}_n}{dr} &= \frac{-n}{k_0^2} \frac{1}{r} \sum_m m (\varepsilon^{-1})_{n-m} H_m + \frac{i\gamma}{\omega \mu_0} \frac{n}{r} \sum_m (\varepsilon^{-1})_{n-m} \tilde{E}_m + r H_n . \end{aligned} \right.$$